



# Observations of phytoplankton productivity and growth rates in the Malin shelf break environment

Stuart C. Painter\*

National Oceanography Centre, Southampton, SO14 3ZH, UK

## ARTICLE INFO

### Keywords:

Malin shelf  
Primary production  
Growth rate  
Productivity  
Cross-shelf exchange

## ABSTRACT

The southern sector of the Malin Shelf, a subregion of the NW European Shelf, is noted for episodic and unimpeded incursions of oceanic water onto the shelf in an area where the northward flowing European slope current interacts with steep bathymetry, yet the in-situ biological consequences of these incursions are largely unexplored. In this study phytoplankton productivity, nitrate assimilation and community growth rates are presented to characterise in-situ biological conditions during a prominent chlorophyll bloom that occurred at the shelf break in July 2013. Surface waters were replete with nitrate ( $2\text{--}7\ \mu\text{mol L}^{-1}$ ) and phosphate ( $0.1\text{--}0.4\ \mu\text{mol L}^{-1}$ ) but deficient in silicate ( $\text{Si} < 1\ \mu\text{mol L}^{-1}$ ). Chlorophyll concentrations were significantly negatively correlated with phosphate concentrations but not correlated with nitrate or silicate. High variability between stations in productivity, nitrate assimilation, and depth averaged phytoplankton community growth rates, which ranged from  $<0.01$  to  $0.14\ \text{d}^{-1}$ , could be attributed to subsurface gradients in production and biomass distributions. Though variable the magnitude of productivity rates in this sector of the Malin Shelf environment do not appear unusual relative to comparable observations suggesting that despite the uncommon physical conditions of the study site phytoplankton productivity was not significantly modified by proximity to oceanic influences.

## 1. Introduction

Located to the north of Ireland and to the west of Scotland, the Malin-Hebrides shelf is a westward facing subregion of the broader NW European Shelf that is exposed to the eastern North Atlantic Ocean (Ellett 1979; McKay et al., 1986; Painter et al., 2016; Porter et al., 2018; Jones et al., 2020). Despite its orientation interactions between the northward flowing European Slope Current and the continental slope, prevalent along-shelf flows, and a prominent shelf break front, are generally sufficient to prevent direct exchange between the Malin-Hebrides shelf and the ocean (Huthnance and Gould, 1989; Pingree et al., 1999; Huthnance 2010; Jones et al., 2020; Huthnance et al., 2022). This leads to sharp gradients across the shelf break in phytoplankton community structure (Gowen et al., 1998; Siemering et al., 2016), inorganic nutrients (Painter et al., 2016), organic nutrients (Moschonas et al., 2015) and dissolved iron concentrations (Birchill et al., 2019). Nevertheless, at the southern end of the Malin Shelf hydrographic observations reveal the presence of unmodified high salinity oceanic water on the shelf (Ellett 1979; McKay et al., 1986; Jones et al., 2020), whilst drogoue tracks also repeatedly demonstrate significant movement of floats released seaward of the shelf

break on to the shelf (Booth and Meldrum, 1987; Porter et al., 2018). Such observations support theoretical arguments that unimpeded ocean-to-shelf exchange can occur in this region (Hill 1995), with the main pathway for inflowing oceanic water identified between  $55$  and  $56^\circ\text{N}$  in the vicinity of a canyon system and steep topography (Hill 1995; White and Bowyer, 1997; Gowen et al., 1998; Porter et al., 2018). Influxes of oceanic water across the shelf break are important for supplying nutrients to support primary production both in the receiving coastal waters of the Malin-Hebrides shelf and more generally across the wider NW European Shelf system due to the clockwise circulation pattern and connectivity of the Malin Shelf with the wider shelf region including the North Sea (Inall et al., 2009; Jones et al., 2020). Yet, locations where unimpeded fluxes of oceanic water occur are considered unusual and it has been shown that oceanic nutrient resupply to the NW European Shelf, particularly during winter, appears limited to, and largely dependent upon, a region southwest of the Celtic Sea (south of Ireland) and to the Malin Shelf (north of Ireland) (Hydes et al., 2004; Heath and Beare, 2008).

Satellite observations of surface chlorophyll or calcite reflectance meanwhile have long demonstrated a sharp boundary between the open

\* Corresponding author.

E-mail address: [stuart.painter@noc.ac.uk](mailto:stuart.painter@noc.ac.uk).

<https://doi.org/10.1016/j.csr.2024.105281>

Received 27 February 2024; Received in revised form 29 May 2024; Accepted 1 July 2024

Available online 2 July 2024

0278-4343/© 2024 The Author. Published by Elsevier Ltd. This is an open access article under the CC BY license (<http://creativecommons.org/licenses/by/4.0/>).

ocean and the Malin Shelf that closely follows the shelf edge (Holligan and Groom 1986; O'Boyle and Silke 2009). Along the southern Malin shelf however this boundary is weaker and high chlorophyll patches can occasionally be observed across the outer shelf (e.g. Fig. 1) suggesting localised enhancement of productivity, presumably in response to nutrient resupply, yet in-situ observations are limited. Indeed, phytoplankton and productivity studies for the Malin shelf are rather infrequent compared to hydrographic investigations leading to significant temporal intervals between studies (Fehling et al., 2012; Siemering et al., 2016). In this study I pose the question whether phytoplankton productivity and growth rates in the southern Malin shelf region could be influenced by proximity to oceanic influxes and considered in some way different to those reported from neighbouring shelf break environments. Observations of primary production, nitrate uptake and phytoplankton community growth rates and environmental conditions are presented to better understand the biological conditions in the shelf break region associated with a summertime high chlorophyll patch that is suspected to have resulted from a nutrient resupply event.

## 2. Methods

### 2.1. Sampling

Sampling was conducted along the Malin Shelf edge during July 2013 on board the *R.R.S. James Cook* (cruise JC088). Six productivity stations were sampled along two hydrographic transects at the shelf break, coincident with high chlorophyll conditions (Fig. 1), with transect locations defined by local bathymetric considerations. Sampled depths for productivity measurements corresponded to surface, 55%, 20%, 7%, 4.5% and 1% of surface irradiance intensities whilst other sampling depths across the upper 200 m followed standard depths. All sampling was conducted with a Seabird 9/11+ CTD/rosette Niskin system with dissolved oxygen and salinity sensors calibrated against discrete samples as per standard oceanographic practice (Hood et al., 2010). Mixed layer depth estimates were calculated using the density threshold method of de Boyer Montegut et al. (2004).

### 2.2. Nutrients

Water samples collected by the hydrographic CTD/Niskin rosette casts were sampled in triplicate into 60 ml HDPE bottles and analysed onboard for dissolved inorganic nutrient concentrations within 2 h of collection. A Bran and Luebbe QuAatro 5-channel nutrient auto-analyser was used following recommended methodologies (Hydes et al., 2010; Becker et al., 2020). Detection limits were  $0.1 \mu\text{mol L}^{-1}$  for total nitrate (nitrate + nitrite),  $0.05 \mu\text{mol L}^{-1}$  for nitrite,  $0.05 \mu\text{mol L}^{-1}$  for phosphate and  $0.1 \mu\text{mol L}^{-1}$  for silicate. Reported concentrations are the means of triplicate analyses.

### 2.3. Particulate concentrations

Ambient particulate organic carbon and nitrogen concentrations were obtained by filtering 1.2 L of seawater from each sampled productivity depth onto ashed ( $450^\circ\text{C}$ ,  $>4$  h) glass fibre filters (Whatman GF/F). After filtration filters were oven dried at  $50^\circ\text{C}$  for 24 h before being placed in 2 ml cryovials and stored at room temperature for subsequent analysis. On land filters were fumed for 24hrs with concentrated HCL acid to remove inorganic carbon before being redried and pelleted into tin capsules. Samples were analysed for carbon, nitrogen and isotopic content on a PDZ Europa ANCA-GSL elemental analyser coupled to a PDZ Europa 20-20 mass spectrometer at the Scottish Association for Marine Sciences (Oban, UK).

### 2.4. Chlorophyll concentrations

Chlorophyll-a concentrations were obtained using the fluorometric method of Welschmeyer (1994). At each sampled depth 250 ml of seawater was filtered onto a 25 mm glass fibre filter (GF/F grade), placed into 6 ml of 90% acetone (HPLC-grade) and stored in the dark for 18–20 h before the extracted fluorescence was measured on a Turner Trilogy fluorometer calibrated against a spinach standard (spinach extract Sigma C5753).

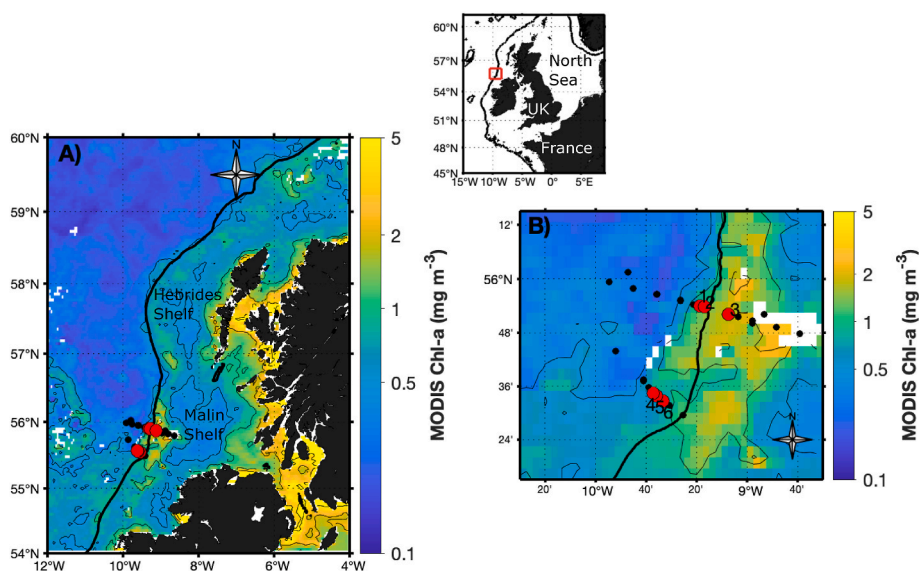


**Fig. 1.** Maps of the study site with MODIS-Aqua mean monthly surface chlorophyll concentrations for July 2013. Panel A shows the study site and sampled stations in the wider context of the Malin-Hebrides shelf system. Note the isolated patch of elevated chlorophyll concentrations at the shelf break. Panel B shows the location of primary production stations (red circles) and other sampled stations (black circles) along two transects across the Malin Shelf break (thick black line) in relation to a prominent region of high surface chlorophyll. Chlorophyll contours in both panels represent the identified contours on the colour scale. Productivity stations are numbered offshore to inshore (1–3 north transect, 4 to 6 south transect). Inset map illustrates study location relative to United Kingdom and Ireland, red box illustrates area shown in panel B.

## 2.5. Primary production and nitrate uptake

Primary production and nitrate uptake were measured using a dual  $^{13}\text{C}/^{15}\text{N}$  labelling methodology (Dugdale and Goering 1967; Slawyk et al., 1977; Hama et al., 1983). At each euphotic depth 1.2 L of seawater was carefully measured into a clear polycarbonate bottle and spiked with  $105 \mu\text{mol L}^{-1}$  of  $^{13}\text{C}$ -labelled sodium bicarbonate enriching the ambient DIC pool to  $\sim 6.1\%$ . A further  $100 \text{ nmol L}^{-1}$  of  $^{15}\text{N}$ -labelled potassium nitrate was added to each bottle leading to a maximum enrichment of  $5.5\%$  compared to ambient nitrate concentrations. All bottles were incubated using deck incubators flushed with surface seawater for 5 h before being filtered onto ashed GF/F filters. Filters were rinsed with  $0.1\text{N HCl}$  to remove inorganic carbon and then with distilled water before being oven dried and stored in cyrovials. In the laboratory the entire filter was pelleted and analysed on the same EA-IRMS system as detailed above to obtain the carbon, nitrogen and respective isotopic contents.

Primary production rates ( $P$ ;  $\text{mg C m}^{-3} \text{ d}^{-1}$ ) were calculated with the equations of Hama et al. (1983).

$$P = \frac{\Delta\text{POC}}{t} \times f \quad [1]$$

Where  $\Delta\text{POC}$  is the change in POC concentration during the incubation,  $t$  is the incubation length (in days) and  $f$  is the discrimination factor for  $^{13}\text{C}$  which was set equal to 1 (IOCCG, 2022). The change in POC is calculated as

$$\Delta\text{POC} = \text{POC} \times \frac{(a_{is} - a_{ns})}{(a_{ic} - a_{ns})} \quad [2]$$

Where POC is the measured POC content of the sample,  $a_{is}$  is the measured  $^{13}\text{C}$  atom percentage of the sample,  $a_{ns}$  is the  $^{13}\text{C}$  natural abundance (in this case taken as the average of separate unlabelled POC samples and set to  $1.0882\%$ ), and  $a_{ic}$  is the atom percent of the enriched DIC pool ( $6.07\%$ ). Integrated productivity rates were obtained by trapezoidal integration.

Nitrate uptake rates were estimated with the equations described by Dugdale and Wilkerson (1986).

$$\rho\text{NO}_3 = \frac{R_{\text{PON}} \text{PON}}{R_{\text{NO}_3} t} \quad [4]$$

where  $\rho\text{NO}_3$  is nitrate uptake,  $R_{\text{PON}}$  is the excess at% enrichment in PON at the end of the incubation, PON is the final particulate organic nitrogen concentration,  $R_{\text{NO}_3}$  is the at% enrichment of the  $\text{NO}_3$  pool and  $t$  is the incubation time.

## 2.6. Phytoplankton growth rates

Phytoplankton growth rates were calculated following Maranon (2005).

$$\mu = \frac{P^B}{C : \text{Chl}} \quad [3]$$

where  $P^B$  is the primary production rate per unit chl- $a$  ( $\text{mg C} [\text{mg Chl-}a]^{-1} \text{ d}^{-1}$ ) and  $C:\text{Chl}$  is the carbon to chlorophyll ratio ( $\text{mg C} [\text{mg chl-}a]^{-1}$ )

## 2.7. Statistical analysis

Pearson's correlation was used to identify relationships between environmental and biological variables. Differences between transects were assessed via a Kruskal-Wallis test. All statistical analysis was conducted in R (version 4.2.3 (R Core Team 2024)) with a significance criterion set to 0.05.

## 3. Results

### 3.1. Northern transect

#### 3.1.1. Environmental conditions

Along the northern transect chlorophyll concentrations exhibited a seaward decrease becoming increasingly patchy once past the shelf break (Fig. 2). Maximum chlorophyll concentrations along this transect were  $>2 \text{ mg m}^{-3}$ . In contrast surface nitrate concentrations increased away from the shelf, ranging from  $<3 \mu\text{mol L}^{-1}$  at the most inshore station to  $\sim 7 \mu\text{mol L}^{-1}$  offshore. Consequently, high chlorophyll conditions were broadly co-located with low to moderate nitrate concentrations. Phosphate and silicate concentrations exhibited opposing patterns, with phosphate concentrations increasing from  $<0.2 \mu\text{mol L}^{-1}$  onshore to  $\sim 0.4 \mu\text{mol L}^{-1}$  offshore, whilst surface silicate concentrations were low but generally  $>0.5 \mu\text{mol L}^{-1}$  except for the most offshore stations where concentrations fell to  $\sim 0.1 \mu\text{mol L}^{-1}$ . Surface temperatures ranged from  $\sim 13.7^\circ\text{C}$  to  $15.7^\circ\text{C}$  and were higher at the inshore end of the transect. Surface salinity was largely invariant along the transect with values of  $35.5 \text{ g kg}^{-1}$ , with indications of a weak freshening at the inshore end of the transect where salinity reduced to  $35.4 \text{ g kg}^{-1}$ . The density section indicated the presence of stratified conditions across the outer shelf but also that stratification became progressively weaker once past the shelf break. Mixed layer depths along the transect ranged from 12 to 18 m (mean  $\pm$  S.D. of  $15.4 \pm 2.7$  m). Daily averaged wind speeds during the occupation of the northern transect ranged from  $6.2$  to  $13.2 \text{ m s}^{-1}$ .

#### 3.1.2. Primary production, nitrate uptake and phytoplankton growth rates

The productivity stations along the northern transect were located close to the shelf break and in waters with comparable surface environmental conditions (e.g. mixed layer depths of 14–18 m, nitrate and phosphate concentrations of  $5.56$ – $5.77 \mu\text{mol L}^{-1}$  and  $0.24$ – $0.36 \mu\text{mol L}^{-1}$  respectively) but exhibited rather different productivity patterns (Table 1). Surface chlorophyll concentrations varied 2.5 fold between stations whilst particulate C and N pools varied 3.8–4.5-fold respectively and surface primary production rates exhibited almost 400-fold differences. Differences in particulate C:N stoichiometry were far less variable between stations (range 6.3–7.4), but indicated a higher C:N at the inshore station suggesting a minor shift toward lower overall N content. The highest surface productivity rate of  $37 \text{ mg C m}^{-3} \text{ d}^{-1}$  was observed at the inshore station 3, where nitrate uptake was also highest ( $77.7 \text{ nmol N L}^{-1} \text{ hr}^{-1}$ ), but productivity and nitrate uptake rates were otherwise considerably lower along this transect ( $<2.3 \text{ mg C m}^{-3} \text{ d}^{-1}$  and  $<0.9 \text{ nmol N L}^{-1} \text{ hr}^{-1}$ ). Phytoplankton growth rates were also highest inshore ( $0.12 \text{ d}^{-1}$ ) and decreased offshore ( $<0.01 \text{ d}^{-1}$ ), a pattern that was comparable to the offshore gradient in chlorophyll concentrations (Table 1).

#### 3.1.3. Integrated and depth averaged rates

Integrated nutrient and chlorophyll concentrations and depth averaged growth conditions are summarised in Table 2. Euphotic zone (0–45 m) integrated nutrient pools revealed comparable nitrate ( $235$ – $253 \text{ mmol NO}_3 \text{ m}^2$ ) and silicate pools ( $28.3$ – $36.5 \text{ mmol Si m}^{-2}$ ) between stations but notably the integrated phosphate pool was  $\sim 30\%$  lower at inshore station 3 ( $10.8$  vs  $14.3$ – $15.2 \text{ mmol PO}_4^{3-} \text{ m}^{-2}$ ). Station 3 also had the highest biomass concentrations (both chl- $a$  and POC/PON) and integrated nitrate uptake rate but not the highest integrated primary production rate which was located at station 2. The depth averaged growth rate at station 3 ( $0.05 \text{ d}^{-1}$ ) was comparable to that found at offshore station 1 ( $0.04 \text{ d}^{-1}$ ), whilst the highest depth averaged growth rate of  $0.1 \text{ d}^{-1}$  was found at station 2, coincidentally the station with the highest integrated primary production rate of  $534 \text{ mg C m}^{-2} \text{ d}^{-1}$ .

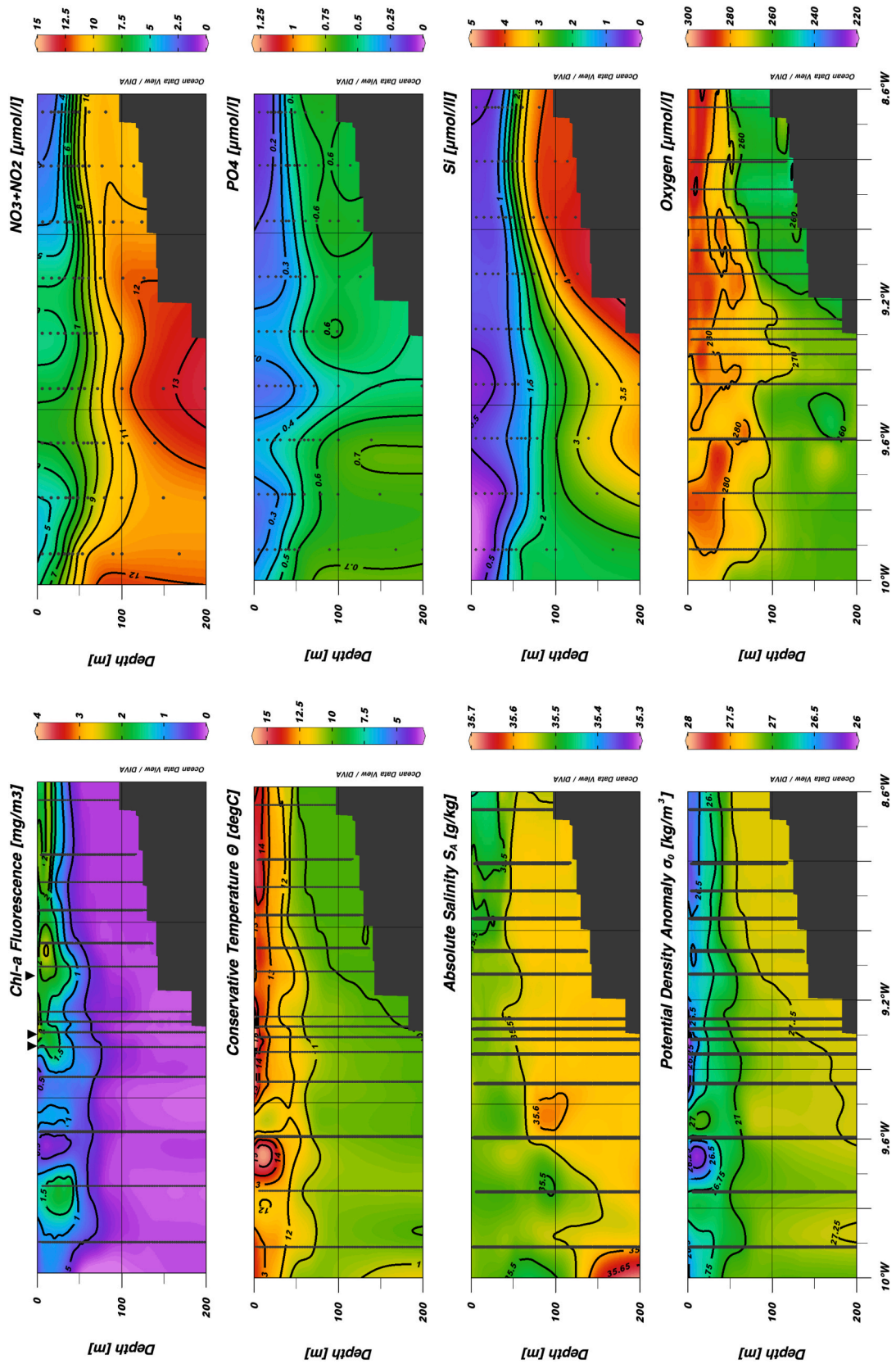


Fig. 2. Contoured sections (0–200 m) along the northern transect showing chlorophyll-a fluorescence (calibrated against in-situ bottle samples;  $y = x * 1.1707$ ,  $R^2 = 0.979$ ), conservative temperature, absolute salinity, potential density anomaly, nitrate ( $\text{NO}_3 + \text{NO}_2$ ), phosphate ( $\text{PO}_4$ ), silicate (Si) and dissolved oxygen (calibrated against in-situ bottle samples;  $y = 0.927x - 4.5318$ ,  $R^2 = 0.981$ ). Black triangles along top axis of the chlorophyll section denote productivity sampling stations 1 (offshore) to 3 (inshore).

**Table 1**  
 Sampling locations and surface ocean concentrations of nutrients, chlorophyll, particulates and phytoplankton productivity and growth rate estimates. Station numbers as indicated on Fig. 1 (stations 1–3 North transect, 4–6 South transect). Abbreviations used in column headers are POC (particulate organic carbon), PON (particulate organic nitrogen), PP (primary production),  $\rho\text{NO}_3$  (nitrate uptake),  $P_B$  (chlorophyll normalised production) and  $\mu$  (growth rate).

Surface																		
Stn.	Date	Lat (N)	Lon (E)	Water depth (m)	$\text{NO}_2$ ( $\mu\text{M}$ )	$\text{NO}_3+\text{NO}_2$ ( $\mu\text{M}$ )	$\text{NO}_3$ ( $\mu\text{M}$ )	$\text{PO}_4$ ( $\mu\text{M}$ )	Si ( $\mu\text{M}$ )	Chl- <i>a</i> (mg/ $\text{m}^3$ )	POC ( $\mu\text{M}$ )	PON ( $\mu\text{M}$ )	Particulate C: N (molar)	PP (mg C $\text{m}^{-3} \text{d}^{-1}$ )	$\rho\text{NO}_3$ (nmol N $\text{L}^{-1} \text{hr}^{-1}$ )	$P_B$ (mg C [mg chl- <i>a</i> ] $\text{d}^{-1}$ )	C:Chl (mg C [mg Chl- <i>a</i> ] $\text{d}^{-1}$ )	$\mu$ ( $\text{d}^{-1}$ )
1	03/07/2013	55.899	-9.313	575	0.17	5.94	5.77	0.34	0.63	0.87	8.32	1.29	6.4	0.1	0.4	0.1	127.4	0.001
2	04/07/2013	55.896	-9.283	378	0.16	5.72	5.56	0.36	0.69	0.87	10.38	1.65	6.3	2.2	0.9	2.6	163.8	0.02
3	21/07/2013	55.869	-9.124	159	0.51	6.21	5.7	0.24	0.82	2.17	36.55	4.93	7.4	37.0	77.7	17.1	143.1	0.12
<b>Mean <math>\pm</math>SD</b>					0.28 $\pm$ 0.2	5.96 $\pm$ 0.25	5.68 $\pm$ 0.11	0.31 $\pm$ 0.06	0.71 $\pm$ 0.1	1.3 $\pm$ 0.75	18.4 $\pm$ 15.7	2.6 $\pm$ 2.0	6.7 $\pm$ 0.6	13.1 $\pm$ 20.7	26.3 $\pm$ 44.5	6.6 $\pm$ 9.2	144.7 $\pm$ 18.2	0.05 $\pm$ 0.06
4	18/07/2013	55.573	-9.620	1175	0.4	2.21	1.81	0.11	0.44	1.82	9.93	1.61	6.2	16.8	0.5	9.3	67.3	0.14
5	17/07/2013	55.564	-9.598	994	0.21	3.89	3.68	0.24	0.52	1.07	17.25	2.49	6.9	16.3	6.3	15.3	210.7	0.07
6	12/07/2013	55.546	-9.554	586	0.17	3.87	3.7	0.24	0.49	1.27	6.32	0.87	7.2	2.6	0.9	2.1	74.8	0.03
<b>Mean <math>\pm</math>SD</b>					0.26 $\pm$ 0.12	3.32 $\pm$ 0.96	3.06 $\pm$ 1.09	0.2 $\pm$ 0.08	0.48 $\pm$ 0.04	1.39 $\pm$ 0.39	11.2 $\pm$ 5.6	1.7 $\pm$ 0.8	6.8 $\pm$ 0.6	11.9 $\pm$ 8.0	2.6 $\pm$ 3.2	8.9 $\pm$ 6.6	117.6 $\pm$ 80.7	0.08 $\pm$ 0.06

**Table 2**

Integrated results (0–43 m) for nutrients, chlorophyll, particulates and productivity rates. Depth averaged phytoplankton growth rates and particulate pools are also presented. Abbreviations used in column headers are described as per Table 1.

Stn.	Integrated										Depth averaged			
	NO <sub>2</sub> (mmol/ m <sup>2</sup> )	NO <sub>3</sub> +NO <sub>2</sub> (mmol/m <sup>2</sup> )	NO <sub>3</sub> (mmol/ m <sup>2</sup> )	PO <sub>4</sub> (mmol/ m <sup>2</sup> )	Si (mmol/ m <sup>2</sup> )	Chl- $\alpha$ (mg/ m <sup>2</sup> )	POC (mmol/ m <sup>2</sup> )	PON (mmol/ m <sup>2</sup> )	PP (mg C m <sup>-2</sup> d <sup>-1</sup> )	$\rho$ NO <sub>3</sub> (mmol N m <sup>-2</sup> d <sup>-1</sup> )	P <sub>B</sub> (mg C [mg Chl-a] d <sup>-1</sup> )	C:Chl (mg C [mg Chl- $\alpha$ ] d <sup>-1</sup> )	$\mu$ (d <sup>-1</sup> )	Particulate C:N (molar)
1	7.5	250.7	243.3	14.3	28.3	39.0	566.2	93.2	186.7	1.3	4.8	130.0	0.04	6.4
2	7.2	242.4	235.2	15.2	30.4	39.0	411.1	65.3	534.4	3.6	12.8	145.2	0.10	6.3
3	22.0	263.9	241.9	10.9	36.5	74.1	811.0	104.0	491.1	17.5	6.6	110.3	0.05	8.0
<b>Mean</b>	12.3 $\pm$	252.4 $\pm$	240.1	13.4 $\pm$	31.7 $\pm$	50.7	596.1	87.5 $\pm$	404.0	7.4 $\pm$	8.1 $\pm$	128.5	0.06	6.9 $\pm$ 0.9
<b><math>\pm</math>SD</b>	8.5	10.8	$\pm$ 4.3	2.3	4.3	$\pm$	$\pm$ 201.6	19.9	$\pm$	8.7	4.2	$\pm$ 17.5	$\pm$	
						20.3			189.5				0.03	
4	14.9	169.2	154.3	9.3	23.5	64.0	390.1	61.8	357.4	1.7	5.8	168.2	0.07	6.3
5	8.9	204.3	195.4	12.6	26.3	49.4	549.3	74.3	314.8	2.9	7.3	154.9	0.04	7.4
6	7.5	204.5	197.0	12.8	24.8	64.7	495.0	68.7	918.7	7.7	13.5	99.0	0.13	7.3
<b>Mean</b>	10.4 $\pm$	192.7 $\pm$	182.2	12.0 $\pm$	24.9 $\pm$	59.4	478.2	68.3 $\pm$	530.3	4.1 $\pm$	8.8 $\pm$	140.7	0.08	6.9 $\pm$ 0.6
<b><math>\pm</math>SD</b>	3.9	20.3	$\pm$ 24.2	2.0	1.4	$\pm$ 8.6	$\pm$ 80.9	6.3	$\pm$	3.2	4.1	$\pm$ 36.7	$\pm$	
									337.1				0.04	

### 3.2. Southern transect

#### 3.2.1. Environmental conditions

Chlorophyll concentrations along the southern transect exceed 2.5 mg m<sup>-3</sup> at the shelf break, becoming more patchy in their distribution offshore but remaining above 1 mg m<sup>-3</sup> at all stations (Fig. 3). Surface nutrient concentrations were more variable between stations along this transect but overall were <4  $\mu$ mol NO<sub>3</sub> L<sup>-1</sup>, <0.25  $\mu$ mol PO<sub>4</sub> L<sup>-1</sup> and <0.5  $\mu$ mol Si L<sup>-1</sup>. Temperature and salinity distributions revealed homogenous surface conditions with surface temperatures of 14.4–14.8 °C, and salinities of ~35.5 g kg<sup>-1</sup>. The hydrographic conditions along the southern transect were far less variable with depth compared to the northern transect resulting in comparably weaker vertical density gradients. Mixed layer depths were comparable to the northern transect with a similar range of 12–18 m but with a marginally shallower average mixed layer depth overall compared to the northern transect (mean  $\pm$  S.D. of 14.5  $\pm$  2.0 m). Daily averaged wind speeds during the occupation of the southern transect ranged from 3.4 to 9.4 m s<sup>-1</sup>.

#### 3.2.2. Primary production, nitrate uptake and phytoplankton growth rates

The productivity stations on the southern transect had comparable mixed layer depths of 12–14 m, but sharply contrasting environmental conditions with nitrate and phosphate concentrations varying almost 2-fold between stations (2.2–3.9  $\mu$ mol L<sup>-1</sup> and 1.8–3.7  $\mu$ mol L<sup>-1</sup> respectively) whilst silicate concentrations were more consistent (0.4–0.5  $\mu$ mol L<sup>-1</sup>; Table 1). Chlorophyll and particulate concentrations were also variable between stations with a 1.7-fold difference in surface chlorophyll concentrations (1.1–1.8 mg m<sup>-3</sup>), and a 2–3-fold variation in surface POC and PON pools (6.3–17.3  $\mu$ mol C L<sup>-1</sup> and 0.9–2.5  $\mu$ mol N L<sup>-1</sup> respectively). The particulate C:N molar ratio ranged from 6.2 to 7.2, and was highest at the shelf break inshore station. Surface primary production rates were similar between station 4 and 5 (16.3–16.8 mg C m<sup>-3</sup> d<sup>-1</sup>) with both stations exhibiting higher rates of production than station 6 (2.6 mg C m<sup>-3</sup> d<sup>-1</sup>). Surface nitrate uptake rates were also variable between stations yet did not follow the same distribution as primary production with station 4 and 6 being more comparable to each other (0.47–0.92 nmol N L<sup>-1</sup> hr<sup>-1</sup>) and substantially lower than station 5 (6.3 nmol N L<sup>-1</sup> hr<sup>-1</sup>). Surface community growth rates ranged from 0.03 to 0.14 d<sup>-1</sup>, with the highest rate measured at offshore station 4. As with the northern transect the highest growth rate of 0.14 d<sup>-1</sup> was found coincident with the highest surface chlorophyll concentration.

#### 3.2.3. Integrated and depth averaged rates

Euphotic zone integrated and depth averaged growth conditions for the southern transect were also variable between stations (Table 2). Integrated nitrate and phosphate concentrations were ~20–25% lower at station 4 compared to stations 5 and 6, whereas integrated silicate concentrations differed between stations by 10% at most. Integrated chlorophyll concentrations were ~25% lower at station 5 (~49 vs ~64 mg m<sup>-2</sup>), whilst integrated POC and PON concentrations were up to 40% higher at station 5 compared to stations 4 and 6. Integrated productivity rates ranged from 314 to 918 mg C m<sup>-2</sup> d<sup>-1</sup>, whilst integrated nitrate uptake rates ranged from 1.68 to 7.69 mmol N m<sup>-2</sup> d<sup>-1</sup>. Depth averaged growth rates ranged from 0.04 to 0.13 d<sup>-1</sup>, with the highest growth rate observed at station 6, coincident with the highest integrated primary production.

#### 3.2.4. Differences between transects

The productivity profiles for each station are shown in Fig. 4. Stations 1, 2, 5 & 6 all indicate the presence of a subsurface chlorophyll maximum at around 15m depth, and coincident with typical mixed layer depths. Chlorophyll concentrations at the subsurface maximum were 28%–98% higher than corresponding surface concentrations, exceeding 2.5 mg m<sup>-3</sup> at station 6, and being otherwise lower (~1.5–2 mg m<sup>-3</sup>). Station 1 and 2 also exhibited a deeper peak in chlorophyll concentrations at the base of the euphotic zone (~45m). Stations 3 and 4 exhibited a gradual decrease in chlorophyll concentrations from the surface to the base of the euphotic zone. Individual nitrate uptake rates ranged from 0.2 to 77.7 nmol N L<sup>-1</sup> hr<sup>-1</sup>, but with the exception of stations 3 and 6 were generally <6.4 nmol N L<sup>-1</sup> hr<sup>-1</sup> (Table 3). At station 3 the highest recorded uptake rate was almost 6-fold higher than the next highest uptake rate from station 6. Some stations showed the presence of a mid-water column peak in nitrate uptake (e.g. stn. 6), whilst others indicated a deeper maxima (stn 1, 2, 4; Fig. 4). The range in primary production rates was comparable between stations (0.1–40.1 mg C m<sup>-3</sup> d<sup>-1</sup>). Despite the exceptional nitrate uptake rate recorded at station 3 the maximum primary production rate (37 mg C m<sup>-3</sup> d<sup>-1</sup>) for this station was not the highest recorded which was found at station 6. Indeed, other than high nitrate uptake station 3 ultimately exhibited modest phytoplankton growth and chlorophyll normalised productivity rates (Table 3). Overall, the vertical profiles of primary production and nitrate uptake broadly tracked one another suggesting that nitrate was an important driver of productivity.

#### 3.2.5. Statistical analysis

All nutrients tended towards a negative correlation with temperature

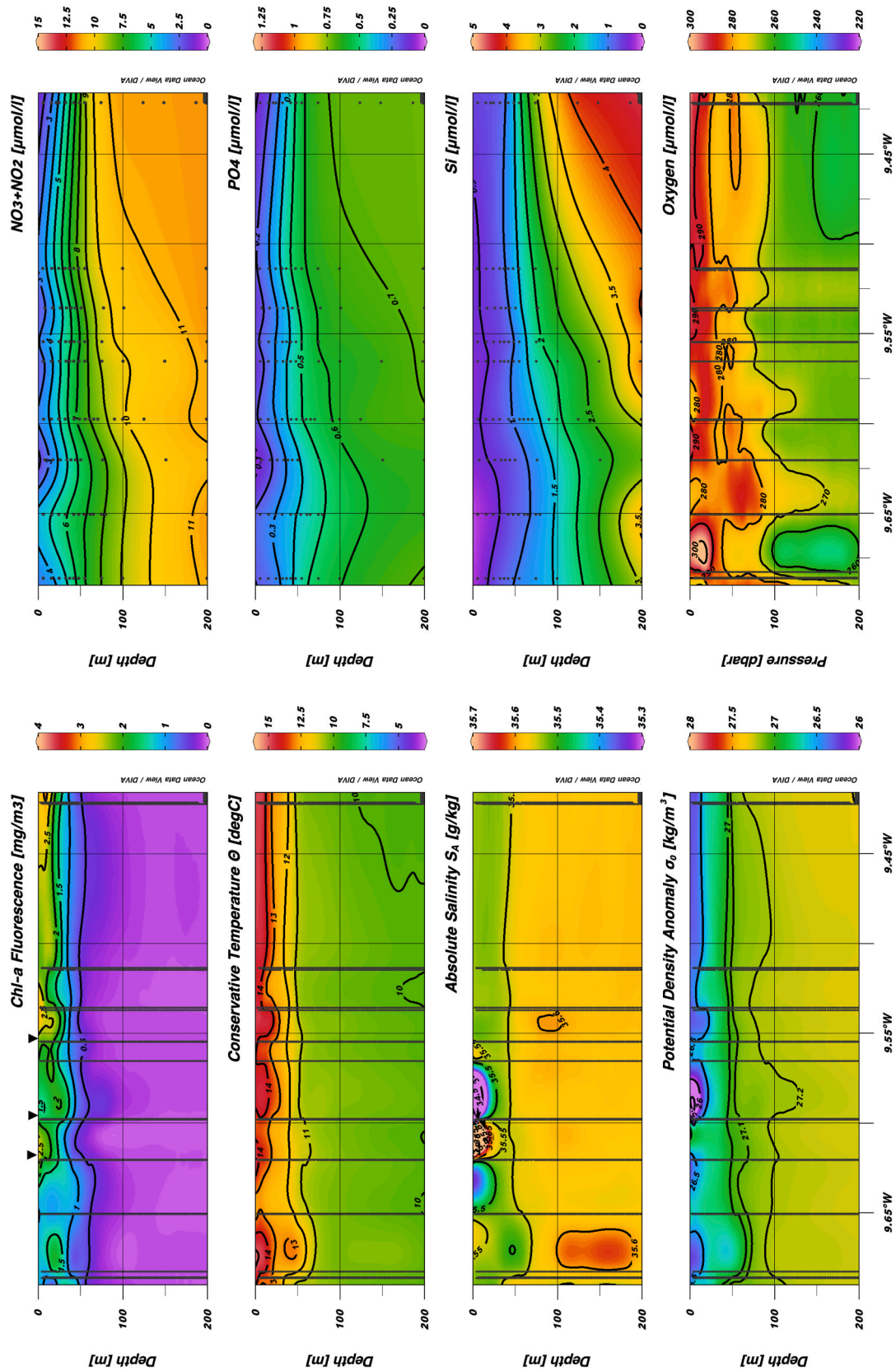
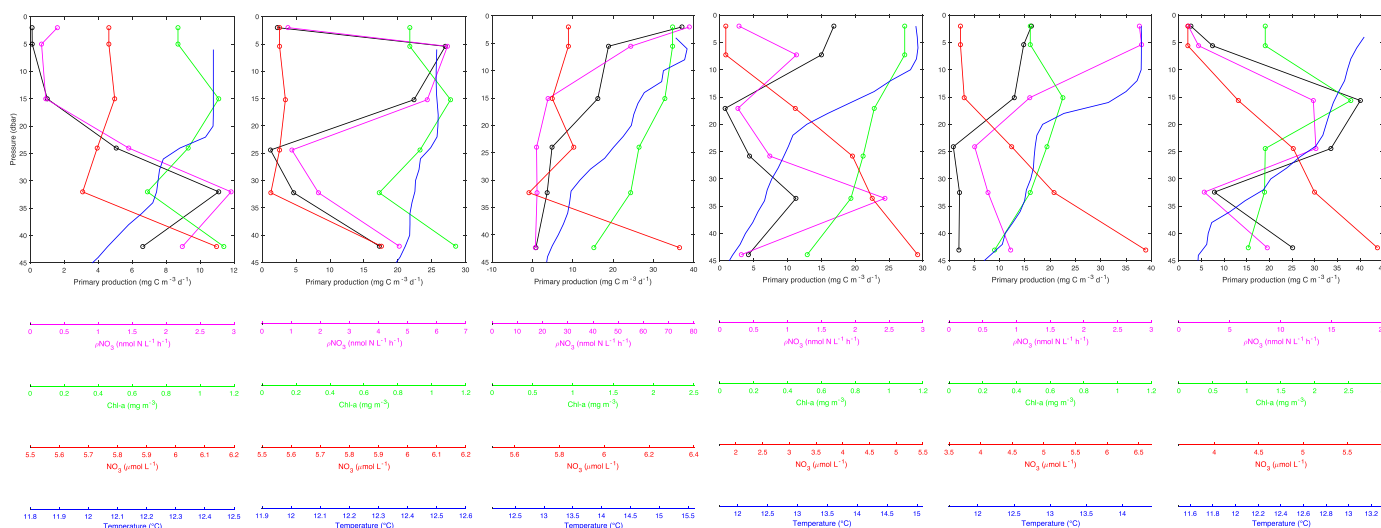


Fig. 3. Contoured sections (0–200 m) along the southern transect showing chlorophyll-a fluorescence, conservative temperature, absolute salinity, potential density anomaly, nitrate ( $\text{NO}_3+\text{NO}_2$ ), phosphate ( $\text{PO}_4$ ), silicate (Si) and dissolved oxygen. Black triangles along top axis of the chlorophyll section denote productivity sampling stations 4 (offshore) to 6 (inshore).



**Fig. 4.** Productivity profiles from the six productivity stations. Profiles are presented for stations 1 to 6 (left to right) and show rates of primary production (black line, black axis), nitrate uptake (magenta line, magenta axis), chlorophyll-a concentration (green line, green axis), nitrate concentration (red line, red axis) and temperature (blue line, blue axis).

**Table 3**  
Range (min-max) of observed productivity variables across the euphotic zone (0–43 m).

Stn.	PP (mg C m <sup>-3</sup> d <sup>-1</sup> )	ρNO <sub>3</sub> (nmol N L <sup>-1</sup> hr <sup>-1</sup> )	μ (d <sup>-1</sup> )	Chl-a (mg/m <sup>3</sup> )	P <sub>B</sub> (mg C [mg chl-a] d <sup>-1</sup> )
1	0.11–11.1	0.17–2.96	<0.01–0.1	0.69–1.14	0.12–16.1
2	1.23–26.97	0.89–6.37	0.01–0.21	0.69–1.14	1.33–31.07
3	0.84–37.04	1.4–77.74	0.01–0.12	0.95–2.17	0.88–17.05
4	0.77–16.83	0.44–4.06	0.01–0.14	0.86–1.82	0.51–9.26
5	0.84–16.28	0.84–6.34	0.01–0.07	0.6–1.50	0.65–15.27
6	2.63–40.06	0.92–13.44	0.03–0.22	1.02–2.53	2.06–26.41

but only the relationship between phosphate and temperature proved significant ( $r = -0.8$ ,  $p < 0.001$ ) (Fig. 5). Phosphate was also significantly negatively correlated with chlorophyll ( $r = -0.67$ ,  $p < 0.001$ ) whilst chlorophyll itself was positively correlated with temperature ( $r = 0.71$ ,  $p < 0.001$ ). Chlorophyll was not significantly correlated with primary production, nitrate uptake, nitrate or silicate concentrations. Primary production was correlated with nitrate uptake ( $r = 0.59$ ,  $p < 0.05$ ) but not with ambient nitrate concentrations.

The mean conditions along both transects of almost all variables were found to be comparable with only integrated nitrate and silicate pools being significantly different (Table 2;  $H(1) = 3.85$ ,  $p < 0.05$ ). These significant differences were also evident in the surface nutrient data (Table 1;  $H(1) = 3.85$ ,  $p < 0.05$ ), which are reflective of mixed layer conditions - noting that the mixed layer was shallower than the euphotic depth. Hence it was concluded that the mixed layer along the northern transect was significantly enriched in nitrate and silicate compared to the southern transect. Primary production and nitrate uptake were however broadly comparable between transects but surface productivity and nitrate uptake rates at station 3 were significantly higher than the average ( $t$ -test,  $t = -4.26$ ,  $p < 0.05$  and  $t = -4.93$ ,  $p < 0.05$  respectively). Integrated nitrate uptake at station 3 ( $t = -4.66$ ,  $p < 0.05$ ) and integrated primary production at station 6 ( $t = -4.35$ ,  $p < 0.05$ ) were also higher than average.

**4. Discussion**

Two closely located transects were sampled in summer 2013 within the Malin shelf break environment. The results revealed similarities and differences between stations that are relevant to ongoing efforts to understand phytoplankton productivity and growth at the shelf edge. Differences between individual productivity stations included contrasting chlorophyll-a, nutrient and particulate concentrations, and differences in primary production and nitrate uptake rates. Such variability is consistent with limited previous observation of nutrients and phytoplankton from this region (e.g. (Gowen et al., 1998; Hydes et al., 2004; Scherer and Gowen 2013; Siemerling et al., 2016; Painter et al., 2017)). Stations with the highest surface community growth rates were spatially decoupled from stations with the highest depth-averaged community growth rates, a pattern attributable to subsurface gradients and particularly to the presence or absence of a subsurface chlorophyll maximum.

Despite sampling during July when strong thermal stratification and low nutrient concentrations may be expected surface waters were

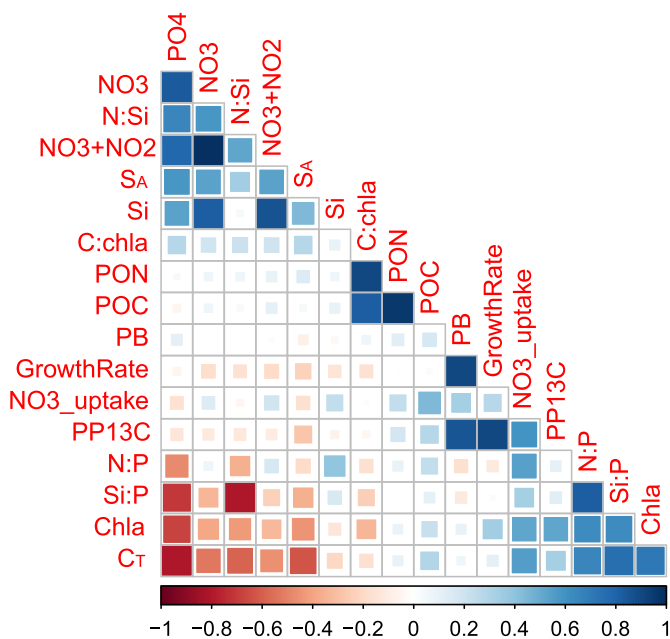


**Fig. 5.** Correlation analysis matrix showing strength of correlations between environmental and biotic variables. Negative correlations indicated in red, positive correlations indicated in blue.

replete with nitrate with concentrations of 2.9–7.2  $\mu\text{mol NO}_3 \text{ L}^{-1}$  along the northern transect and 2.1–4.6  $\mu\text{mol NO}_3 \text{ L}^{-1}$  along the southern transect. Such concentrations are lower than winter concentrations of 10–11  $\mu\text{mol NO}_3 \text{ L}^{-1}$  reported for the Malin shelf edge environment (Hydes et al., 2004; Scherer and Gowen, 2013) but higher than reported previously for this region when surface concentrations at the shelf edge in July 2012 peaked at 2.8  $\mu\text{mol NO}_3 \text{ L}^{-1}$  and were otherwise  $<0.5 \mu\text{mol NO}_3 \text{ L}^{-1}$  across the outer shelf (Scherer and Gowen, 2013). Along the northern transect there was evidence of upward isopycnal displacement at the shelf edge (Fig. 2), whilst along the southern transect nitrate isopleths moved closer to the surface as the shelf break was approached (Fig. 3), suggesting a possible source for the nutrients.

Notwithstanding the elevated summertime nitrate concentrations the integrated primary production rates of 0.18–0.92  $\text{g C m}^{-2} \text{ d}^{-1}$  (Table 2) were broadly consistent with typical rates of  $\sim 0.5 \text{ g C m}^{-2} \text{ d}^{-1}$  reported from stratified regions of the wider NW European Shelf (Holligan 1989) and to summertime rates of  $<0.4 \text{ g C m}^{-2} \text{ d}^{-1}$  reported from the Celtic Sea shelf break environment (Joint et al., 2001; Poulton et al., 2019). Nevertheless, the highest primary production rate of 0.92  $\text{g C m}^{-2} \text{ d}^{-1}$ , which was almost twice the next largest rate (0.53  $\text{g C m}^{-2} \text{ d}^{-1}$ ), does appear elevated suggesting localised enhancement of productivity in the shelf break region, which at this time was on the periphery of a high chlorophyll patch (Fig. 1). The integrated productivity rates were also comparable to summertime rates of 0.1–0.5  $\text{g C m}^{-2} \text{ d}^{-1}$  and 0.2–0.7  $\text{g C m}^{-2} \text{ d}^{-1}$  reported from the central Celtic Sea away from the shelf break by Hickman et al. (2012) and Poulton et al. (2019) respectively implying that the highest observed rate may not be that elevated. Unlike these previous results however, the productivity stations in this study were located within waters of relatively high nitrate concentrations. A possible reason for the apparent lack of productivity, despite residual nitrate being available, may be found in the N:Si and Si:P ratios which revealed that all stations exhibited signs of Si deficiency across the euphotic zone (e.g. Si:P  $< 5$ ), due to low surface silicate concentrations (0.5–1  $\mu\text{mol Si L}^{-1}$ ). As sampling occurred after the earlier spring bloom this is perhaps unsurprising but Si deficiency relative to other nutrients may be a condition that is common throughout the year for this shelf system (Painter et al., 2017). Most sampled depths exhibited balanced N:P conditions ( $\text{NO}_3:\text{PO}_4$ ) relative to an approximation of 16:1 for balanced growth (Redfield 1958) with only samples within the upper 25 m at station 5 and samples from station 6 indicating a minor to moderate phosphorous deficiency when N:P ratios reached 18 to 26. This suggests that  $\text{PO}_4$  availability was not generally a limiting factor. Winter N:P conditions of 16–16.6 have been reported at the Malin shelf edge, with lower values of  $\sim 14$  across the inner shelf, indicating a moderate phosphorous excess (relative to nitrogen) away from the shelf break at the start of the productive period (Hydes et al., 2004). Based on the cyclical pattern in nutrient stoichiometry described by Painter et al. (2017) for the Malin-Hebrides shelf system the timing of these productivity observations should have coincided with the slow transition from a post spring bloom P deficient system (high N:P) to an N deficient system reflective of stratified summer conditions (low N:P). This was not the case and the combination of higher surface nitrate concentrations than reported previously, in-situ N:P values comparable to winter values, and elevated chlorophyll concentrations likely signifies localised vertical mixing and nutrient resupply. Any such mixing however does not appear to have impacted silicate concentrations, with the highest subsurface concentrations found not at the shelf edge but in the benthic layer of the shelf itself, presumably due to remineralization of spring bloom generated biomass (Fig. 2).

The range of individual growth rates reported here (0.0–0.22  $\text{d}^{-1}$ ; Table 3) are in keeping with comparable studies from temperate shelf regions, which range from 0.0 to 3.4  $\text{d}^{-1}$  (Furnas 1990), yet the maximum growth rate is towards the lower end of these previous rate estimates. The maximum rate is also lower than reported for the Celtic Sea (1.3  $\text{d}^{-1}$  (Geider 1988);). The highest surface phytoplankton growth rates (0.12–0.14  $\text{d}^{-1}$ ) were found at stations displaying the highest

chlorophyll-a concentrations (1.8–2.2  $\text{mg m}^{-3}$ ). Primary production rates provided only marginal diagnostic support for the distribution of maximum phytoplankton growth with two comparably productive stations (4 and 5) on the southern transect displaying a 2-fold variation in surface growth rates, a possible consequence of modest P limitation as indicated by elevated N:P ratios in the upper euphotic zone at station 5, or to changes in the phytoplankton community between stations. In contrast the highest depth averaged phytoplankton growth rates (0.1–0.13  $\text{d}^{-1}$ ) were found at stations with the highest integrated rates of primary production. No single station displayed both high surface and high depth averaged growth rates highlighting the importance of sub-surface biomass distributions. Overall, there was high spatial variability over where maximum productivity or where maximum growth rates could be found. The occurrence of a high depth averaged growth rate at station 6 in waters displaying both Si limitation and a high N:P ratio indicative of growing P deficiency suggests that P availability may play a key role in setting in-situ growth rates. Previous studies have demonstrated seasonality in phosphorous uptake dynamics within a shelf sea setting which includes the onset of high biomass normalised phosphorous uptake during summer when phosphorous is usually limiting (Poulton et al., 2019). Strong gradients in dissolved iron across the Malin shelf edge have also been reported (Birchill et al., 2019).

Nitrate uptake profiles broadly followed productivity profiles (Fig. 4), but whilst high integrated nitrate uptake did not necessarily co-occur with high integrated primary production it did co-occur with the highest integrated chlorophyll-a concentrations. This indicates a role for other nitrogenous nutrients in supporting primary production in the shelf break environment, for example ammonium (e.g. (Joint et al., 2001).

Whilst the focus here has been on (macro)nutrient forcing of phytoplankton growth rates, other factors that may be relevant to the interpretation of the productivity data, but which cannot be resolved beyond a general discussion, should be mentioned. These include grazing, mixing and advection processes, wind speeds and surface currents. Wind speeds during the cruise were light to moderate but were stronger earlier in the cruise when daily average wind speeds exceeded 10  $\text{m s}^{-1}$ , compared to speeds of  $<6 \text{ m s}^{-1}$  later in the cruise. Wind directions were southerly to south westerly but during the primary productivity sampling at station 6 winds veered from the southeast (and were weaker). The impact of temporally weakening winds and shifting wind directions on the reported productivity rates is unclear. The large scale advective circulation for this shelf region is well described (e.g. (Jones et al., 2020)) and generally acts to move water along the shelf edge or away from the shelf edge in a northeasterly direction. Indeed, drogued drifters released during this cruise passed through the study region in a northeasterly direction with velocities of  $\sim 10 \text{ cm s}^{-1}$  (Jones et al., 2020) implying that advective losses of phytoplankton biomass away from the shelf break may occur, with the general advective direction potentially also explaining the orientation of the observed high chlorophyll patch (Fig. 1). Supporting measurements of grazing rates are not available and the impact of grazing on productivity rates remains uncertain. Further work is therefore required.

Finally, the dataset presented here is small and offers only a simple snapshot of a temperate frontal region in summer but nevertheless the data illustrates the magnitude and variability of biological and environmental conditions. For the majority of stations the biological conditions appear broadly comparable to the neighbouring Celtic Sea shelf break, another region where ocean to shelf exchange has been identified (Hydes et al., 2004; Heath and Beare, 2008) but in general the productivity rates do not appear elevated compared to typical rates for the NW European Shelf. This suggests that despite the unusual physical setting phytoplankton productivity and growth rates are not unusual. A single station with elevated productivity remains an intriguing outlier in this dataset and may indicate that the region of greatest productivity and growth enhancement lies downstream of the shelf break, where coincidentally the highest satellite chlorophyll concentrations were

observed (Fig. 1). Simple extrapolations from surface chlorophyll distributions as to where maximum phytoplankton growth rates may be found are however clearly complicated by the presence of subsurface chlorophyll or productivity maxima which can decouple maximum surface and depth averaged growth rates.

## 5. Conclusions

Primary productivity and phytoplankton growth rates were investigated in the Malin shelf break environment, a region where unusually the cross-shelf exchange of oceanic waters occurs unimpeded. Despite unexpectedly high surface nitrate concentrations for the time of year in situ primary productivity and phytoplankton growth rates were found comparable to neighbouring shelf regions suggesting no appreciable enhancement in productivity due to the unusual physical setting. High variability in growth rates was however evident between stations though no environmental driver for this was identified. A single station with notably enhanced productivity may indicate that the largest productivity enhancement takes place downstream of the shelf break, a region where coincidentally satellite observations indicate high chlorophyll conditions.

## CRedit authorship contribution statement

**Stuart C. Painter:** Writing – review & editing, Writing – original draft, Supervision, Formal analysis, Conceptualization.

## Declaration of competing interest

The authors declare that they have no known competing financial interests or personal relationships that could have appeared to influence the work reported in this paper.

## Acknowledgements

This study is an output from Fluxes Across Sloping Topography of the North East Atlantic (FASTNET), a project funded by the UK Natural Environment Research Council (NERC) via award NE/1030151/1. This study benefits from Open Data supplied by the Natural Environment Research Council via the British Oceanographic Data Centre ([www.bodc.ac.uk](http://www.bodc.ac.uk)).

I thank Morwenna Cooper and Victoria Hemsley for assistance with sample collection.

## References

IOCCG Protocol Series, 2022. Aquatic Primary Productivity Field Protocols for Satellite Validation and Model Synthesis. In: Balch, W.M., Carranza, M., Cetinic, I., Chaves, J. E., Duhamel, S., Fassbender, A., Fernandez-Carrera, A., Ferrón, S., García-Martín, E., Goes, J., Gomes, H., Gundersen, K., Halsey, K., Hirawake, T., Isada, T., Juranek, L., Kulk, G., Langdon, C., Letelier, R., López-Sandoval, D., Mannino, A., Marra, J.F., Neale, P., Nicholson, D., Silsbe, G., Stanley, R.H., Vandermeulen, R.A. (Eds.), IOCCG Ocean Optics and Biogeochemistry Protocols for Satellite Ocean Colour Sensor Validation, 7.0. IOCCG, Dartmouth, NS, Canada, p. 202. <https://doi.org/10.25607/OBP-1835> edited by R.A. Vandermeulen, J. E. Chaves.

Becker, S., Aoyama, M., Woodward, E.M.S., Bakker, K., Coverly, S., Mahaffey, C., Tanhua, T., 2020. GO-SHIP repeat hydrography nutrient manual: the precise and accurate determination of dissolved inorganic nutrients in seawater, using continuous flow analysis methods. *Front. Mar. Sci.* 7.

Birchill, A.J., Hartner, N.T., Kunde, K., Siemering, B., Daniels, C., Gonzalez-Santana, D., Milne, A., Ussher, S.J., Worsfold, P.J., Leopold, K., Painter, S.C., Lohan, M.C., 2019. The eastern extent of seasonal iron limitation in the high latitude North Atlantic Ocean. *Sci. Rep.* 9, 1435. [10.1038/s41598-019-41018-37436-41593](https://doi.org/10.1038/s41598-019-41018-37436-41593).

Booth, D.A., Meldrum, D.T., 1987. Drifting buoys in the northeast Atlantic. *Journal Conseil International pour l'Exploration de la Mer* 43, 261–267.

de Boyer Montegut, C., Madec, G., Fischer, A.S., Lazar, A., Ludicone, D., 2004. Mixed layer depth over the global ocean: an examination of profile data and a profile-based climatology. *J. Geophys. Res.* 109, C12003. [10.1029/12004JC002378](https://doi.org/10.1029/12004JC002378).

Dugdale, R.C., Goering, J.J., 1967. Uptake of new and regenerated forms of nitrogen in primary productivity. *Limnol. Oceanogr.* 12 (2), 196–206.

Dugdale, R.C., Wilkerson, F.P., 1986. The use of  $^{15}\text{N}$  to measure nitrogen uptake in eutrophic oceans; experimental considerations. *Limnol. Oceanogr.* 31 (4), 673–689.

Ellett, D.J., 1979. Some oceanographic features of Hebridean waters. *Proc. Roy. Soc. Edinb. B Biol. Sci.* 77, 61–74.

Fehling, J., Davidson, K., Bolch, C.J.S., Brand, T.D., Narayanaswamy, B.E., 2012. The relationship between phytoplankton distribution and water column characteristics in north west European shelf sea waters. *PLoS One* 7 (3), e34098.

Furnas, M.J., 1990. In situ growth rates of marine phytoplankton: approaches to measurement, community and species growth rates. *J. Plankton Res.* 12 (6), 1117–1151.

Geider, R.J., 1988. Estimating the growth and loss rates of phytoplankton from time-series observations of  $^{14}\text{C}$  biocarbonate uptake. *Mar. Ecol. Prog. Ser.* 43, 125–138.

Gowen, R.J., Raine, R., Dickey-Collas, M., White, M., 1998. Plankton distributions in relation to physical oceanographic features on the southern Malin Shelf, August 1996. *ICES (Int. Council. Explor. Sea) J. Mar. Sci.* 55, 1095–1111.

Hama, T., Miyazaki, T., Ogawa, Y., Iwakuma, T., Takahashi, M., Otsuki, A., Ichimura, S., 1983. Measurement of photosynthetic production of marine phytoplankton population using a stable  $^{13}\text{C}$  isotope. *Mar. Biol.* 73, 31–36.

Heath, M.R., Beare, D.J., 2008. New primary production in northwest European shelf seas, 1960–2003. *Mar. Ecol. Prog. Ser.* 363, 183–203.

Hickman, A.E., Moore, C.M., Sharples, J., Lucas, M.L., Tilstone, G.H., Krivtsov, V., Holligan, P.M., 2012. Primary production and nitrate uptake within the seasonal thermocline of a stratified shelf sea. *Mar. Ecol. Prog. Ser.* 463, 39–57.

Hill, A.E., 1995. Leakage of barotropic slope currents onto the continental shelf. *J. Phys. Oceanogr.* 25, 1617–1621.

Holligan, P.M., 1989. Primary production in the shelf seas of North-West Europe. *Adv. Bot. Res.* 16, 193–252.

Holligan, P.M., Groom, S.B., 1986. Phytoplankton distributions along the shelf break. *Proceedings Royal Soc. Edinburgh* 88B, 239–263.

Hood, E.M., Sabine, C.L., Sloyan, B.M. (Eds.), 2010. The GO-SHIP Repeat Hydrography Manual: A Collection of Expert Reports and Guidelines. IOCCP Report Number 14, ICPO Publication Series Number 134. Available online at: <http://www.go-ship.org/HydroMan.html>.

Huthnance, J.M., 2010. The northeast Atlantic margins. In: Liu, K.-K., Atkinson, L., Quiñones, R., L. T.M. (Eds.), *Carbon and Nutrient Fluxes in Continental Margins*. Springer-Verlag, Berlin Heidelberg, pp. 215–234.

Huthnance, J.M., Gould, W.J., 1989. On the northeast Atlantic slope current. In: Neshyba, S.J., Mooers, C.N.K., Smith, R.L., Barber, R.T. (Eds.), *Poleward Flows along Eastern Ocean Boundaries*, vol. 34, p. 374. Coastal and Estuarine Studies.

Huthnance, J., Hopkins, J., Berx, B., Dale, A., Holt, J., Hosegood, P., Inall, M., Jones, S., Loveday, B.R., Miller, P.I., Polton, J., Porter, M., Spings, C., 2022. Ocean shelf exchange, NW European shelf seas: measurements, estimates and comparisons. *Prog. Oceanogr.* 202, 102760.

Hydes, D.J., Gowen, R.J., Holliday, N.P., Shammon, T., Mills, D., 2004. External and internal control of winter concentrations of nutrients (N, P and Si) in north-west European shelf seas. *Estuar. Coast Shelf Sci.* 59, 151–161.

Hydes, D.J., Aoyama, M., Aminot, A., Bakker, K., Becker, S., Coverly, S., Daniel, A., Dickson, A.G., Grosso, O., Kerouel, R., van Ooijen, J., Sato, K., Tanhua, T., Woodward, E.M.S., Zhang, J.Z., 2010. Determination of dissolved nutrients (N, P, Si) in seawater with high precision and inter-comparability using gas-segmented continuous flow analysers. The GO-Ship Repeat Hydrography Manual: A collection of expert reports and guidelines 1–87. IOCCP Report No. 14, ICPO Publication Series No. 134. **Version 1, 2010.**

Inall, M., Gillibrand, P., Griffiths, C., MacDougal, N., Blackwell, K., 2009. On the oceanographic variability of the North-West European Shelf to the west of Scotland. *J. Mar. Syst.* 77, 210–226.

Joint, I., Wollast, R., Chou, L., Batten, S., Elskens, M., Edwards, E., Hirst, A., Burkill, P., Groom, S., Gibb, S., Miller, A., Hydes, D., Dehairs, F., Antia, A., Barlow, R., Reesa, A., Pomroy, A., Brockmann, U., Cummings, D., Lampitt, R., Løjens, M., Mantoura, F., Miller, P., Raabe, T., Alvarez-Salgado, X., Stelfox, C., Woolfenden, J., 2001. Pelagic production at the Celtic Sea shelf break. *Deep-Sea Research II* 48, 3049–3081.

Jones, S., Inall, M., Porter, M., Graham, J.A., Cottier, F., 2020. Storm-driven across-shelf oceanic flows into coastal waters. *Ocean Sci.* 16 (2), 389–403.

Maranon, E., 2005. Phytoplankton growth rates in the Atlantic subtropical gyres. *Limnol. Oceanogr.* 50 (1), 299–310.

McKay, W.A., Baxter, J.M., Ellett, D.J., Meldrum, D.T., 1986. Radiocaesium and circulation patterns west of Scotland. *J. Environ. Radioact.* 4, 205–232.

Moschonas, G., Gowen, R.J., Stewart, B.M., Davidson, K., 2015. Nitrogen dynamics in the Irish Sea and adjacent shelf waters: an exploration of dissolved organic nitrogen. *Estuar. Coast Shelf Sci.* 164, 276–287.

O'Boyle, S., Silke, J., 2009. A review of phytoplankton ecology in estuarine and coastal waters around Ireland. *J. Plankton Res.* 32 (1), 99–118.

Painter, S.C., Hartman, S.E., Kivimäe, C., Salt, L.A., Clargo, N.M., Bozec, Y., Daniels, C.J., Jones, S.C., Hemsley, V.S., Munns, L.R., Allen, S.R., 2016. Carbon exchange between a shelf sea and the ocean: the Hebrides Shelf, west of Scotland. *J. Geophys. Res.* 121, 4522–4544. [10.1002/2015JC011599](https://doi.org/10.1002/2015JC011599).

Painter, S.C., Hartman, S.E., Kivimäe, C., Salt, L.A., Clargo, N.M., Daniels, C.J., Bozec, Y., Daniels, L., Allen, S., Hemsley, V.S., Moschonas, G., Davidson, K., 2017. The elemental stoichiometry (C, Si, N, P) of the Hebrides Shelf and its role in carbon export. *Prog. Oceanogr.* 159, 154–177.

Pingree, R.D., Sinha, B., Griffiths, C.R., 1999. Seasonality of the European slope current (Goban Spur) and ocean margin exchange. *Continental Shelf Res.* 19, 929–975.

Porter, M., Dale, A.C., Jones, S., Siemering, B., Inall, M.E., 2018. Cross-slope flow in the Atlantic Inflow Current driven by the on-shelf deflection of a slope current. *Deep Sea Res. Oceanogr. Res. Pap.* 140, 173–185.

Poulton, A.J., Davis, C.E., Daniels, C.J., Mayers, K.M.J., Harris, C., Tarran, G.A., Widdicombe, C.E., Woodward, E.M.S., 2019. Seasonal phosphorus and carbon dynamics in a temperate shelf sea (Celtic Sea). *Progress Oceanography* 177, 101872.

- R Core Team, 2024. R: A Language and Environment for Statistical Computing. R Foundation for Statistical Computing, Vienna, Austria. URL. <https://www.R-project.org/>.
- Redfield, A.C., 1958. The biological control of chemical factors in the environment. *Am. Sci.* 46 (3), 205–221.
- Scherer, C., Gowen, R., 2013. Field Surveys of the Malin Shelf Ecosystem in Winter and Summer 2012 and Winter 2013. WP2 of the EFF Project CA/033766/11 35.
- Siemering, B., Bresnan, E., Painter, S.C., Daniels, C.J., Inall, M., Davidson, K., 2016. Phytoplankton distribution in relation to environmental drivers on the North West European shelf sea. *PLoS One* 11 (10), e0164482, 0164410.0161371/journal.pone.0164482.
- Slawyk, G., Collos, Y., Auclair, J., 1977. The use of the  $^{13}\text{C}$  and  $^{15}\text{N}$  isotopes for the simultaneous measurement of carbon and nitrogen turnover rates in marine phytoplankton. *Limnol. Oceanogr.* 22, 925–932.
- Welschmeyer, N.A., 1994. Fluorometric analysis of chlorophyll a in the presence of chlorophyll b and phaeopigments. *Limnol. Oceanogr.* 39 (8), 1985–1992.
- White, M., Bowyer, P., 1997. The shelf-edge current north-west of Ireland. *Ann. Geophys.* 15, 1076–1083.